6284 *Macromolecules* **2010**, *43*, 6284–6294
DOI: 10.1021/ma101013c

Macromolecules
ARTICLE

Importance of Functional Monomer Dimerization in the Molecular Imprinting Process

Yagang Zhang, Di Song, Laura M. Lanni, and Ken D. Shimizu*

Department of Chemistry and Biochemistry, University of South Carolina, Columbia, South Carolina 29208

Received May 10, 2010; Revised Manuscript Received June 21, 2010

ABSTRACT: We examined the influence of functional monomer dimerization on the efficiency of the molecular imprinting process. Specifically, the influence of methacrylic acid (MAA) dimerization on the binding properties of molecularly imprinted polymers (MIPs) was studied. First, the dimerization of MAA and the association between MAA and template molecular ethyl adenine-9-acetate (EA9A) were characterized in solution. Next, a series of MIPs and control nonimprinted polymers (NIPs) were made under varying conditions that systematically disrupted the monomer dimerization and templation process by the addition of polar solvents to the polymerization mixture. The results showed that even a monomer such as MAA with low dimerization constant is able to efficiently suppress the formation of background binding sites. To isolate the influence of monomer dimerization on the imprinting effect, the equilibrium processes in the prepolymerization mixture were modeled using the computer program COPASI. The simulation was able to reproduce the experimentally observed relationship between monomer dimerization and the suppression of the background sites. While monomer dimerization reduced the number of templated sites, the reduction in the number of background sites was large, leading to an overall increase in the percentage of templated sites. In addition, conditions were identified in which MAA dimerization can actually improve the imprinting efficiency as measured by the fraction of selective templated to background sites. On the basis of these studies with MAA, we predict that other functional monomers that can dimerize or aggregate should also show higher imprinting efficiencies in terms of selectivity while sacrificing some binding capacity. Both experimental and simulation results demonstrated that one must be very careful when using NIPs as control systems to characterize the imprinting effect as the suppression of background sites in the NIP can lead to differences in binding capacities of the MIP and NIP even in the absence of an imprinting effect.

Introduction

The molecular imprinting process is a synthetically efficient and low-cost approach for preparing polymers with tailored recognition properties.[1−4] The preparation of molecular imprinted polymers (MIPs) typically involves three steps (Scheme 1). First, a monomer−template complex is formed via self-assembly of monomer and template units. Next, the monomer−template complex is polymerized with an excess of cross-linker to form a rigid polymer monolith. Finally, the template is removed creating binding cavities with shape and functional group complementarily to the template molecule. Because of the efficiency and versatility, the imprinting process has been successfully applied to a wide range of templates, including small molecule drugs,[5] environmental pollutants,[6] herbicides,[7] amino acids,[8] peptides,[9] proteins,[10] nucleotides,[11] and even proteins.[12] MIPs also display excellent thermal, pH, and chemical stabilities, especially in comparison to biological systems.[13] Accordingly, MIPs have been used in a broad range of applications requiring molecular recognition including liquid chromatography,[14,15] drug delivery,[16] catalysis,[1] and solid-phase extraction (SPE)[17,18] and sensing.[19]

The practical utility of MIPs, however, has been limited by their poor to mediocre binding properties. In most cases, the imprinting process proceeds with low fidelity, and thus, only a small fraction of the binding sites possess high affinity and selectivity for the template molecule.[20−22] This leads to overall binding affinities and selectivities that are much lower than comparable biological recognition platforms such as antibodies, enzymes, and aptamers. To address these challenges, considerable effort has been focused on improving the efficiency of the imprinting process. The influence of most of the variables in the imprinting process has been extensively studied and optimized including cross-linking density,[23−25] temperature,[26,27] solvent,[28,29] template aggregation,[30−33] monomer to template ratio,[34,35] and concentration.[36,37] One variable that has only recently been studied is the influence of functional monomer dimerization or aggregation, and this variable has been only studied in the context of computational models of the imprinting process.[38−42] One reason is because one would predict that monomer dimerization should compete with the templation process and should be detrimental to the imprinting process. However, our recent studies using urea-based monomers[43] led us to postulate that functional monomer aggregation might have beneficial effects by suppressing the formation of the nonselective background sites.

Typically, a large excess of functional monomer is used in the imprinting process to drive the formation of the monomer−template complexes (Scheme 2a). One side effect is that the majority of the monomer units are not complexed to templates and, instead, form large numbers of background sites. Monomer dimerization has the potential to reduce the number of these background sites (Scheme 2b). Binding sites formed from the dimerized monomer will, effectively, be deactivated as the recognition groups are blocked by self-association. In looking for monomers to test this hypothesis, we realized that methacrylic acid (MAA) has a strong tendency to form hydrogen-bonded dimers.[38,41,42] Thus, we embarked on a study to assess the

*To whom correspondence should be addressed: Tel 803-777-6523, fax 803-777-9521, e-mail shimizu@chem.sc.edu.

 Published on Web 07/12/2010

Scheme 1. Illustration of the Three-Step Molecular Imprinting Process of Ethyl Adenine-9-acetate (EA9A) within a Methacrylic Acid (MAA)/ Ethylene Glycol Dimethacrylate (EGDMA) Copolymer

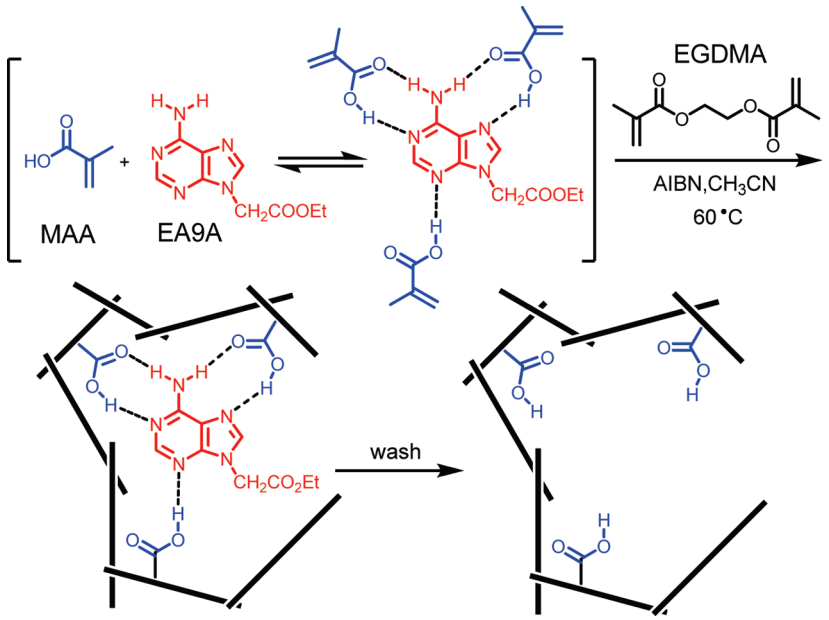

Scheme 2. Illustration Comparing Imprinted (a and b) and Nonimprinted Polymers (c and d) Formed from Functional Monomers That Have or Lack the Ability To Dimerize[a]

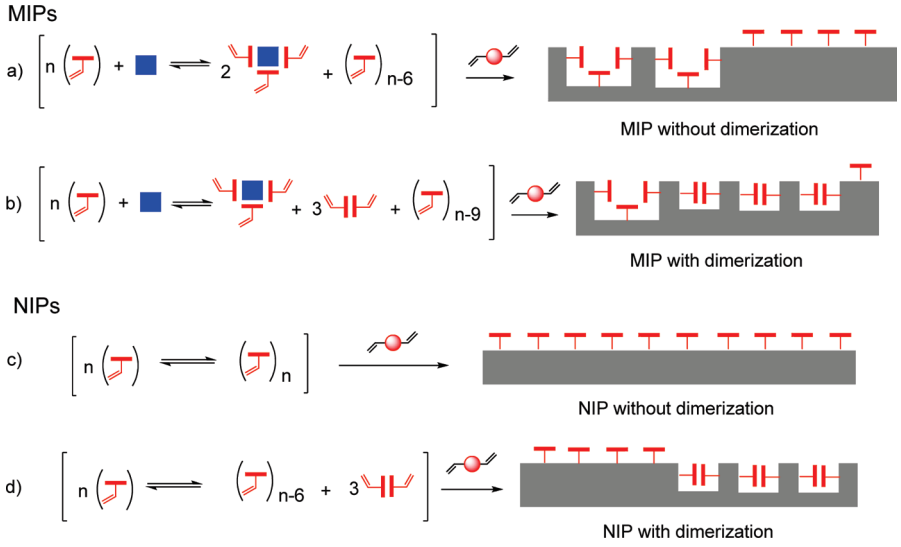

[a] The number of untemplated background sites is predicted to be significantly lower in polymers formed from monomers that can form dimers.

influence of MAA dimerization on the efficiency of the imprinting process. We were particularly interested in whether the ability of MAA to form dimers might help explain its extraordinary success and versatility as an MIP functional monomer.[44]

For this study, a well-studied MAA-based MIP system was chosen (Scheme 1).[45−48] Specifically, the nucleobase, ethyl adenine-9-acetate (EA9A), was imprinted in acetonitrile using MAA as the functional monomer and ethylene glycol dimethacrylate (EGDMA) as the cross-linker.

Our strategy was to characterize the MAA association processes in solution and then to compare binding capacities of polymers formed with varying degrees of MAA dimerization. Finally, we isolated the effects of MAA dimerization on the imprinting process using a computer simulation. Particularly useful were comparisons of the nonimprinted polymers (NIPs) formed in the absence of template that was polymerized in solvents of varying polarity. These allowed for the direct examination of the relationship between of the degree of dimerization and the numbers of background sites (Scheme 2c,d). Also, the computer simulation enabled us to isolate the contributions of monomer dimerization to the imprinting effect. Both the experimental and computational studies agreed that the ability of MAA to form dimers greatly reduces the number of background sites without degrading the efficiency of the imprinting process.

Experimental Section

General. ^{1}H NMR spectra were recorded on a Varian 300 MHz NMR at 21 °C. Chemical shifts (ppm) were referenced to tetramethylsilane or residual protonated solvent. UV measurements were made using a Jasco V-530 spectrometer. Solvents were purified and dried by passing through a PURE SOLV solvent purification system (Innovative Technology). Deuterated solvents were purchased from Cambridge Isotope

Laboratories. All other reagents were purchased from Sigma-Aldrich and were used as received.

NMR Titrations To Obtain Binding Constant of EA9A and MAA. NMR titrations were performed using EA9A and freshly distilled MAA in dry acetonitrile-d_3. To a 700 μL solution of 8.5 mM EA9A were added aliquots of a MAA solution (412 mM). The measured chemical shifts of the EA9A amino protons were fitted to a 1:1 binding model to yield a $K_a = 7.5\ M^{-1}$.[49]

NMR Dilution Experiments To Measure MAA Dimerization Constant. The chemical shift of the carboxylic acidic proton of MAA in acetonitrile-d_3 was measured over the concentration range 0.27−11.1 M. A dimerization constant of 1.9 M^{-1} was calculated by using a numerical curve fitting procedure described by Williams et al. that corrects for variations in chemical shifts that arise from the changes in permittivity at high MAA concentrations.[50]

Preparation−Synthesis of MIPs and NIPs. The synthesis of a representative EA9A-imprinted polymer followed the reported procedure,[2,11] as follows. EA9A (0.025 g, 0.11 mmol), MAA (0.094 g, 1.1 mmol), EGDMA (1.89 g, 9.54 mmol), and AIBN (0.033 g, 0.20 mmol) were dissolved in 2.0 mL of acetonitrile in a screw-capped vial. The mixture was degassed in an ultrasonic bath for 5 min under nitrogen. The vial was sealed then immersed in a water bath at 65 °C for 6 h. The resulting monolith was crushed and ground with a mortar and pestle to a fine powder. The template and the unreacted species were removed by Soxhlet extraction of the polymer particles with methanol for 24 h and then with a mixture of methanol/acetonitrile (1:4 v/v) for another 24 h. The washed polymers were dried overnight under vacuum. A nonimprinted control polymer (NIP) was synthesized following the same protocol but without template.

Batch Binding Studies. For the rebinding studies, 2.5 mL of a 0.1 mM solution of EA9A in acetonitrile was shaken for 2 h with 60 mg of polymer. The solution was filtered to remove all particles, and the absorbance (257 nm) of the supernatant was measured. Background absorbance was measured exactly the same procedure except using 2.5 mL of pure acetonitrile. The percent of EA9A bound by the polymer was determined by the change in absorbance of the supernatant and background absorbances as compared to a stock solution 0.1 mM solution of EA9A in acetonitrile.

Gas Adsorption Porosimetry. The washed and dried polymers (100 mg) were degassed for 16 h at 50 °C and analyzed by nitrogen adsorption porosimetry using a Quantachrome Autosorb automated gas sorption system. Surface areas and average pore diameter were obtained by the Brunauer−Emmett−Teller (BET) method (5 points BET) at 77.35 K.

Imprinting Simulations Using the COPASI Program. COPASI is a software application for simulation and analysis of complex multistep equilibrium.[51] COPASI Version 4.5 was used to simulate the imprinting and dimerization processes in the prepolymerization mixture. The assumption was made that the distributions of various monomer−template complexes in the prepolymerization mixture are representative of those found in the resulting polymerized monolith.[52,53]

In the model, the multiple reversible equilibriums used in the simulation were as shown in eqs 1−4, where M and T are the concentrations of monomer and template, respectively. The template has three identical M binding sites. Therefore, the relationships between K_{a1}, K_{a2}, and K_{a3} are based on the decreasing statistical probability of complex formation on the three binding sites on the template (eq 5). Uncomplexed M forms type 0 binding sites which are defined as nonselective background binding sites. The complex MT forms type 1 binding sites, complex M_2T forms type 2 binding sites, and complex M_3T forms type 3 binding sites. Thus, the numbers of each type of sites are equal to concentration of the corresponding MT species in the prepolymerization solution. Type 1, 2, and 3 binding sites are defined as selective templated binding sites (Scheme 3). The binding energies of the binding sites were assumed to be additive.

Scheme 3. Multiple Equilibrium in Imprinting Process That Form Different Types of Binding Sites[a]

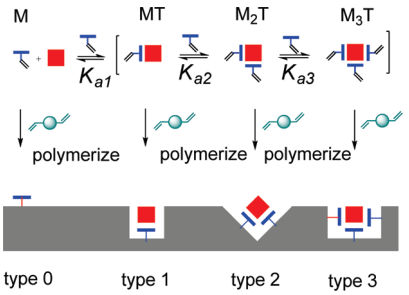

[a] Type 0 is background site; types 1, 2, and 3 are selective sites.

Thus, $K_{(\text{type 1})} = K_a$, $K_{(\text{type 2})} = (K_a)^2$, and $K_{(\text{type 3})} = (K_a)^3$.

$$M + M \rightleftharpoons M_2 \quad (1)$$

$$M + T \rightleftharpoons MT \quad (2)$$

$$MT + M \rightleftharpoons M_2T \quad (3)$$

$$M_2T + M \rightleftharpoons M_3T \quad (4)$$

$$K_{a1}/3 = K_{a2} = 3K_{a3} \quad (5)$$

Results and Discussion

The study of the influence of MAA dimerization was carried out in three parts. First, the monomer−monomer and monomer−template association constants in solution were measured. These studies verified the ability of MAA to dimerize and provided association constants for the later simulations. Next, a series of MIPs and NIPs were made with varying concentrations of polar solvent, which systematically disrupted the dimerization and templation processes. The resulting changes in the binding capacities of the polymers were assessed via batch binding studies. Finally, the influences of monomer dimerization were assessed using computer models that simulated the equilibrium processes in the prepolymerization solution.

Characterization of the MAA Binding Interactions. The ability of carboxylic acids to form hydrogen-bonded dimers has been well established in both solution and the solid-state.[54−57] The stability of the MAA dimer in acetonitrile was measured using ^{1}H NMR dilution studies that followed the chemical shift of the acidic carboxylic acid proton from 11.1 to 0.27 M (Figure 1). In acetonitrile, the K_{dim} of MAA is very low, making accurate measure of the value very difficult. High concentrations of MAA are required to approach saturation, which changes the permittivity of the solution and the observed chemical shift. Using the equilibrium models developed by Williams et al. that take into account variations in permittivity,[50] a dimerization constant of $K_{dim} = 1.9\ M^{-1}$ was measured for MAA in acetonitrile. The importance of using William's models is apparent from the shape of the experimental titration curve at higher MAA concentrations. The curve never appears to reach saturation due to the large changes in permittivity at high MAA concentrations. Using these correction factors, an excellent curve fit of the experimental data was observed (Figure 1).

Table 1. Standard Polymerization Conditions for Formation of EA9A MIP and NIP[a]

polymer	MAA (mmol)	EA9A (mmol)	EGDMA (mmol)	AIBN (mmol)	binding capacity[b] (μmol/g)	surface areas (m^2/g)[c]
MIP	1.10	0.11	9.54	0.2	3.610	460
NIP	1.10		9.54	0.2	0.549	450

[a] The monomer, template, cross-linker, and radical initiator were dissolved in 4 mL of acetonitrile and heated in a sealed vial for 6 h at 65 °C. [b] Binding capacities were measured by equilibrating polymer (60 mg) in acetonitrile solution of EA9A (2.5 mL, 0.1 mM) for 1.5 h. The concentration of unbound EA9A was measured by UV−vis (257 nm). [c] Surface areas and pore diameters were calculated from a multipoint nitrogen adsorption isotherm using a Brunauer−Emmett−Teller model.

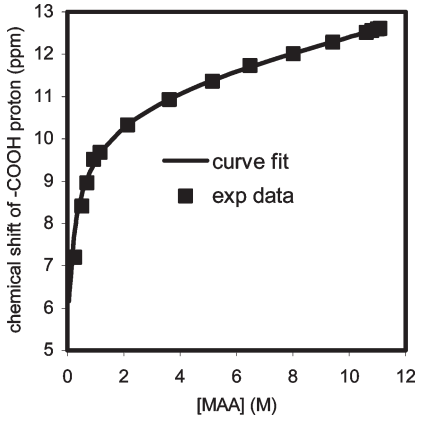

Figure 1. ^{1}H NMR dilution experiment of MAA in CD_3CN measuring the dimerization constant (K_{dim}). The MAA −COOH proton was followed.

The K_{dim} of 1.9 M^{-1} in acetonitrile is higher than the K_{dim} value reported by Ansell[42] (0.33 M^{-1}); this difference is probably due to the different models that were used to curve fit the titration data and methods of analysis.

Characterization of the Monomer−Template Association. The monomer−template interactions between MAA and EA9A were also characterized via ^{1}H NMR titration. Continuous variation analysis (Job's plot) at two different concentrations (8.5 and 2.1 mM) yielded an MAA to EA9A stoichiometry of 1.4:1, which is intermediate between 1:1 and 2:1 (Figure 2). Although carboxylic acids are known to form 2:1 and 3:1 complexes with adenines,[11,45,47,48] lower stoichiometry is due to the low MAA−EA9A association constant in CH_3CN. These studies showed that MAA−EA9A monomer−template complex was stronger than MAA dimer, confirming that the templation process could dominate the dimerization process. The ^{1}H NMR titration experiment (Figure 2) showed the expected upfield shifts of the EA9A amino protons, which is consistent with the formation of a hydrogen-bonded complex of MAA with the Hoogsteen−Watson−Crick faces of adenine. Therefore, the titration data were modeled to a 1:1 binding model yielding an excellent fit and an association constant of K_a = 7.5 M^{-1} ($K_a = K_{a1}$ in Scheme 3).

Next, a series of EA9A-imprinted and nonimprinted polymers were synthesized by using MAA as the functional monomer and EGDMA as the cross-linker. This MIP was chosen for study because it is well studied, easily synthesized from commercially available starting materials, and straightforward to characterize the binding properties using UV−vis spectroscopy. The polymers were polymerized in acetonitrile using AIBN as a radical initiator at 65 °C for 6 h. The high 10:1 monomer/template ratios was used to ensure the formation of the MAA−EA9A complexes. A high level of 87% cross-linking was used to ensure the formation of rigid polymer matrix. First, a MIP and NIP were synthesized and characterized to measure the magnitude of the imprinting effect. The MIP and NIP formulations are shown in Table 1, and each polymer was thermally polymerized at 65 °C for 6 h in 4 mL of acetonitrile. After

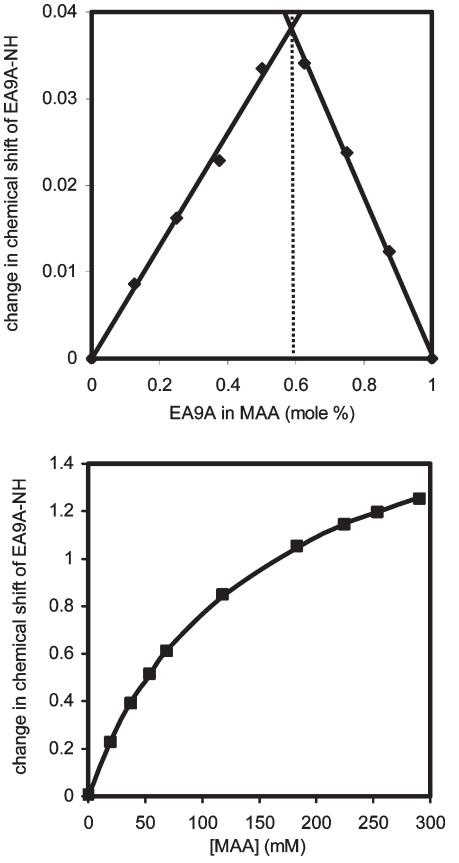

Figure 2. Job's plot for MAA and EA9A at 8.5 mM CD_3CN showing a MAA to EA9A stoichiometry of 1.4:1 (top) by monitoring chemical shifts of the EA9A amino protons and ^{1}H NMR titration curve of the addition of MAA to EA9A in CD_3CN (bottom). The measured chemical shifts of the EA9A amino protons were fitted to a 1:1 binding model to yield a K_a = 7.5 M^{-1}.

polymerization, the insoluble polymer monoliths were ground to a fine powder, washed extensively by Soxhlet extraction, and dried under vacuum.

Batch binding studies of the MIP and NIP were carried out by equilibrating 60 mg of polymer in 2.5 mL of 0.1 mM EA9A−acetonitrile solution (Table 1). Comparison of the data provides evidence for a strong imprinting effect as the MIP had a binding capacity that was 7 times higher than the NIP (3.61 μmol/g vs 0.51 μmol/g). To rule out the possibility that these differences were due to differences in morphology, the BET surface areas of the MIP and NIP were measured. The high surface areas of the NIP (460 m^2/g) and MIP (450 m^2/g) were consistent with the formation of mesoporous monoliths.[58] The similarity in the surface areas and pore diameters (not shown) of the MIP and NIP confirms that the differences in binding capacity are not due to differences in morphology.

Effect of Adding Polar Solvent upon Dimerization and Monomer−Template Complex Formation. To test whether monomer dimerization could reduce the number of background sites, a series of MIPs and NIPs were prepared in

Table 2. Polymerization Conditions for EA9A MIPs and NIPs Formed in the Presence of Varying Percentage of Polar Solvent Additives, AcOH, and MeOH[a,b]

polymer	functional monomer (mmol)	template (mmol)	polymerization solvent[c]
MIP(AcOH)	MAA (1.10)	EA9A (0.11)	AcOH in CH_3CN (0−25% v/v)
MIP(MeOH)	MAA (1.10)	EA9A (0.11)	MeOH in CH_3CN (0−50% v/v)
NIP(AcOH)	MAA (1.10)		AcOH in CH_3CN (0−25% v/v)
NIP(MeOH)	MAA (1.10)		MeOH in CH_3CN (0−50% v/v)
TEA−NIP(AcOH)	MAA (1.10)	TEA (5.50)	AcOH in CH_3CN (0−25% v/v)

[a] The monomer, template, cross-linker, and radical initiator were dissolved in 4 mL of solvent and heated in a sealed vial for 6 h at 65 °C. [b] For each polymer, 9.54 mmol of cross-linker EGDMA and 0.20 mmol of initiator AIBN were used. [c] Total volume solvent was 4.0 mL to prepare each polymer.

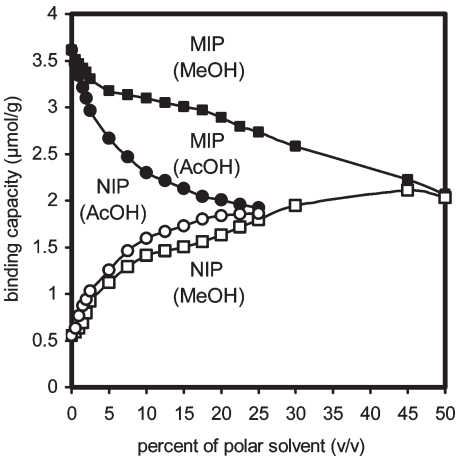

Figure 3. Binding capacities for EA9A of a series MIPs and NIPs polymerized in acetonitrile solutions containing varying percentages of methanol or acetic acid.

acetonitrile solutions containing increasing concentrations of a second more polar solvent (Table 2). Two different polar additives were used: AcOH and MeOH. The polar solvent additives systematically disrupt the formation of the hydrogen-bonded MAA dimers and MAA−EA9A complexes in the prepolymerization mixtures. Therefore, a comparison of the binding capacities of the polymers provides a measure of the role of these association processes in the formation of background and templated binding sites.

The binding capacities of the polymers for EA9A are shown in Figure 3. As expected, the largest differences in binding capacity of the MIPs and NIPs were observed for polymers prepared in the absence of the polar solvent additives (0% v/v polar solvent). As the concentrations of AcOH and MeOH in the polymerization solutions increased, the differences in binding capacities of the MIPs and NIPs narrowed to the point where they became identical. The steady decrease in binding capacity of the MIPs with increasing MeOH and AcOH concentrations was consistent with previous studies that have shown that the imprinting process is much less efficient in polar solvents.[59,60] The common explanation is that polar solvents disrupt the formation of the monomer−template complexes, resulting in fewer imprinted binding sites.

More intriguing was that the opposite trend that was observed in the NIPs. The binding capacities of the NIPs steadily increased with increasing concentrations of the polar solvent additives. The much higher binding capacities of the NIPs formed in more polar solutions are not readily explained by simple imprinting models as there was no template in the prepolymerization solutions. However, it is consistent with our hypothesis that the formation of MAA dimers in the prepolymerization solution can suppress the formation of non-templated background binding sites. Thus, NIPs formed in the absence of MeOH or AcOH have low binding capacities because MAA is able to efficiently dimerize in pure acetonitrile. This results in a much lower concentration of free MAA units that can form the background binding sites. NIPs formed in more polar solvents have higher binding capacities because the polar solvents destabilize the MAA dimers, leading to an increase in the concentration of free MAA and in the number of the background binding sites.

The efficiency with which MAA dimerization was able to suppress the formation of background binding sites in the NIPs was surprising especially considering the very low MAA dimerization constant in acetonitrile. The binding capacities increased 3-fold from 0.55 μmol/g in pure acetonitrile to 1.9−2.1 μmol/g in an excess of polar solvent additives. This suggests that two-thirds of the potential background binding sites in the NIP were eliminated by MAA dimerization. Estimates of the formation of dimerized MAA units in pure acetonitrile based on the MAA dimerization constant and MAA concentrations showed that even with a MAA dimerization constant of 1.9 M^{-1}, one-third were tied up as dimers in the prepolymerization solution. These analyses will be discussed in more detail in the simulation portion of the study. The high percentage of dimers is due to the high concentrations of MAA in the prepolymerization mixtures (0.2 M), which helps offset the low MAA K_{dim}. In the actual MIPs and NIPs, the fraction of MAA carboxylic acids that are dimerized is probably even higher as the prepolymerization process occurs over hours,[61] and the soluble MAAs in oligomers and polymer chains will have much higher degree of association as they contain multiple MAA−MAA interactions.

To rule out the possibility that the observed changes in binding capacity were due to changes in polymer morphology and surface area, the surface areas and average pore diameters of the MIPs and NIPs were again characterized and compared (Table 3). The analysis showed that polymers formed in the presence and absence of AcOH or MeOH had very similar morphologies and surface areas. For example, MIPs formed in pure CH_3CN and 25% AcOH/CH_3CN had very similar surface areas (450−500 m^2/g) as did the NIPs formed in pure CH_3CN and 25% MeOH/CH_3CN (450−500 m^2/g). The average pore diameters of all the polymers were also very similar. These results helped rule out the possibility that the differences in binding capacity were due to differences in morphology.

Comparison of the shapes of the curves in Figure 3 provides additional insight into relative stabilities of the monomer−template and monomer−monomer complexes. First, the more polar AcOH had a much stronger effect than MeOH, as the carboxylic acids in AcOH is able to make heterodimers with the carboxylic acids in MAA. A prepolymerization solution of 25% v/v AcOH/CH_3CN completely eliminated the imprinting effect, as measured by the difference in binding capacity of the MIP and NIP. In contrast, much higher percentage of MeOH (45% v/v) was required to achieve the same effect. The differences in the influences of the polar solvent additives were consistent with our hypothesis that the polar solvent additives were disrupting MAA association processes, which resulted in polymers of varying binding capacity.

Table 3. Surface Areas, Pore Diameters, and Binding Capacities of MIPs and NIPs[d] Formed in Different Solvent Mixtures

polymer	EA9A (mmol)	polymerization solvent(s)[a]	surface area (m^2/g)[b]	average pore diameter (Å)[b]	binding capacity (μmol/g)[c]
MIP	0.11	CH_3CN	450	80	3.60
MIP(25% AcOH)	0.11	25% v/v AcOH/CH_3CN	500	67	1.90
NIP		CH_3CN	460	72	0.55
NIP(25% MeOH)		25% v/v MeOH/CH_3CN	500	68	1.80

[a] Polymers were polymerized with 0.20 mmol of AIBN in a sealed vial (65 °C, 6 h) in 4 mL of solvent. [b] Surface areas and pore diameters were calculated from a multipoint nitrogen adsorption isotherm using a Brunauer–Emmett–Teller model. [c] Binding capacities for EA9A were measured by the change in the absorption (257 nm) of EA9A acetonitrile solutions (0.1 mM, 2.5 mL) after equilibration with 60 mg of polymer. [d] 1.10 mmol of MAA and 9.54 mmol of EGDMA were used to prepare each polymer.

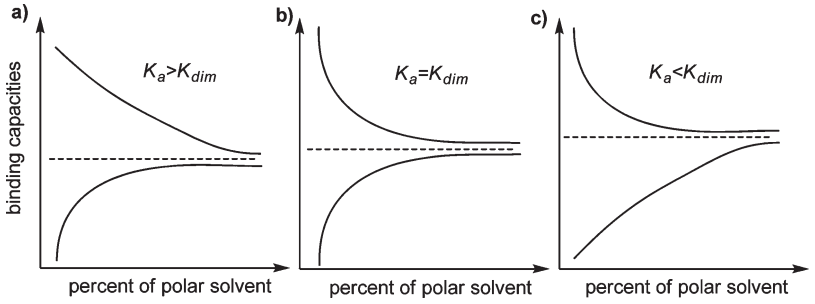

Figure 4. Hypothetical binding capacity curves for MIPs and NIPs made in increasing concentrations of polar solvents, having different relative functional monomer dimerization (K_{dim}) and monomer–template association constants (K_a).

Second, the symmetry or asymmetry of the asymptotic MIP and NIP curves in Figure 3 provides a measure of the relative stabilities of the monomer–monomer (K_{dim}) and monomer–template (K_a) complexes. Three possible scenarios are shown in Figure 4. If $K_a \approx K_{dim}$, then the monomer–monomer and monomer–template complexes should be disrupted to similar extents by the polar solvent additives, and the resulting MIP and NIP binding capacity curves with increasing polar solvent additives should be symmetrical (Figure 4b). Alternatively, if $K_a > K_{dim}$ or $K_a < K_{dim}$, then the MIP and NIP binding capacity curves will be asymmetric (Figure 4a,c), as the lower association constant complexes will be more quickly disrupted by the polar solvent additives and will reach their asymptotic value more quickly. From the measured binding constants, we know that in our system $K_a > K_{dim}$. Yet, the two polar solvent additives MeOH and AcOH appear to correlate to different scenarios of $K_a \approx K_{dim}$ and $K_a > K_{dim}$, respectively. The binding capacity curves for the MeOH polymers are asymmetric and are similar to Figure 4a where $K_a > K_{dim}$. In contrast, the binding capacity curves of the AcOH polymers are symmetrical and are similar to Figure 4b where $K_a \approx K_{dim}$. One explanation of this apparent contradiction is that AcOH is much more polar than MeOH, and thus, AcOH disrupts the monomer–template and monomer–monomer complexes with equal efficiency. The weaker MeOH, however, is able to efficiently disrupt the weak monomer–monomer dimer ($K_{dim} = 1.9\ M^{-1}$) but is not as efficient at disrupting the stronger monomer–template complex ($K_a = 7.5\ M^{-1}$).

Next, a series of NIPs were prepared in the presence of triethylamine (TEA) in order to further test whether the changes in binding capacity of the NIPs were due to changes in the concentrations of MAA dimers. TEA is much more efficient than AcOH or MeOH in disrupting MAA dimerization because TEA forms a strong 1:1 hydrogen-bonded complex with MAA ($K_a = 280\ M^{-1}$ in CH_3CN). Therefore, the addition of only a few equivalents of TEA in the polymerization solution will completely disrupt the MAA dimerization process. More importantly, the low concentrations of TEA have a minimal influence on polymer morphology, and thus, we can eliminate the possibility that differences in binding capacity are due to differences in surface area. The TEA–NIPs were prepared using the same monomer ratios and polymerization conditions as the previous NIPs with the exception of the presence of 5 equiv of TEA (Table 2). For comparison with the previous NIPs, the TEA–NIPs were also prepared in solutions of varying solvent polarity from 0 to 10% v/v AcOH in CH_3CN. The binding capacities of the TEA–NIPs for EA9A were measured and are shown in Figure 5. The very high binding capacities of the TEA–NIPs (1.9 μmol/g) are similar to that of the previous NIPs formed in a large excess of polar solvent additives. This confirms that low concentration of TEA is as effective as very high concentration of AcOH or MeOH in disrupting MAA dimerization, which leads to a stoichiometric formation of background binding sites (Scheme 4).

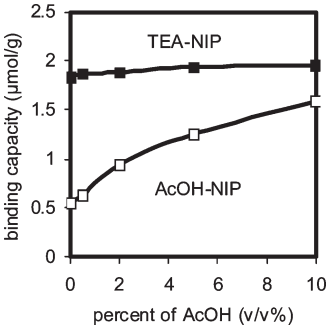

Figure 5. Comparison of the binding capacities for EA9A of TEA–NIPs and NIPs formed in AcOH/CH_3CN.

The unchanging binding capacity of the TEA–NIPs observed in solutions of increasing solvent polarity suggested that TEA efficiently disrupted the MAA dimers, and thus, the MAA dimer concentration could not decrease further with increasing solvent polarity as was observed for the previous NIPs.

The large differences in binding capacity of the NIPs in this study demonstrate that one must be very careful when using NIPs as control systems to characterize the imprinting effect. For example, a common method for verifying and measuring magnitude of the imprinting effect is to measure the difference in binding capacity between an MIP and NIP. The assumption is that the difference in binding capacity arises from enhanced binding capacity of the MIP. However, the above study demonstrates that differences in the MIP

Scheme 4. Illustration of a Nonimprinted Polymer Made with MAA and Triethylamine (TEA) Which Efficiently Disrupts MAA Dimerization, Leading to High Binding Capacity Due to the Stoichiometric Formation of Background Sites

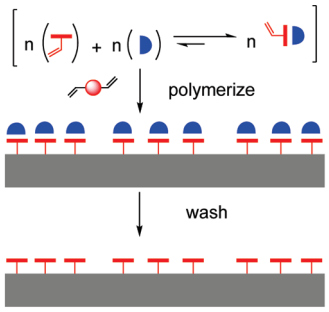

and NIP could also be due to differences in the extent of functional monomer dimerization, which could lead to the inaccurate assignment or overestimation of the imprinting effect. For example, the much higher binding capacity of the NIP−TEA over the NIP could be easily interpreted as arising from the imprinting effect of the TEA template. However, our studies have established that the difference in binding capacity is not due to the enhanced binding properties of the NIP−TEA formed in pure CH_3CN but rather to the suppression of binding sites in the NIP by MAA dimerization. The observation that MIPs formed with an alternative template are often superior controls polymers than NIPs formed in the absence of any template has been recognized from empirical studies of MIPs. For example, in an early report by Spivak and Shea, polymers formed with the benzylamine were used as control polymers for MIP imprinted with 9-ethyladenine as NIPs formed in the absence of any template had such poor binding capacity that the innate affinities of the polymer matrix could not be accurately measured.[47]

General Computational Strategy. A key limitation in our studies into the role of MAA dimerization in the imprinting process is the difficulty in interpreting changes in the binding capacities of the MIPs. MIPs contain both templated and background sites. Thus, the observed decrease in binding capacity of the MIPs formed in more polar solvents could be due to a decrease in the number of templated, background, or both types of binding sites. These scenarios are not easily differentiated because of the difficulties in accurately measuring the populations of the different types of sites in MIPs.[62] In addition, the MAA dimerization and MAA−template association processes are coupled to each other as they both compete for the free MAA. Thus, MAA dimerization will suppress not only the formation of background sites but also the formation of templated sites.

To isolate the effects of functional monomer dimerization on the imprinting process, we turned to computational simulations of the imprinting process. In the simulations, the influence of monomer dimerization on the numbers of imprinted and background sites could be easily assessed. In addition, the dimerization and templation processes could be separately turned on and off. We were particularly interested in answering the question of whether the detrimental effects of MAA dimerization such as the reduction in overall binding capacity were offset by an increase in the ratio of templated to background sites. We were also interested in examining how the relative magnitudes of the monomer dimerization (K_{dim}) and monomer−template complexation (K_a) constants would change efficiency of the imprinting process.

The simulation was based on the premise that imprinted polymers represent a frozen snapshot of the equilibrium processes in the prepolymerization solution. Therefore, by calculating the concentrations of the various species in the prepolymerization solution, the numbers of template imprinted sites and untemplated background sites in the MIPs can be predicted. Free uncomplexed monomer forms the background (type 0) binding sites (Scheme 3). Monomer−template complexes form imprinted binding sites of varying affinity depending upon their stoichiometry. Thus, 1:1 monomer−template complexes form the weakest types of imprinted (type 1) sites and higher order 2:1 and 3:1 monomer−template complexes form the higher affinity (types 2 and 3) imprinted sites.

These types of equilibrium-based simulations of the imprinting process have been successful in predicting the experimentally observed effect of major variables such as solvent polarity,[63−65] association constants,[53] monomer−template stoichiometry,[66−69] and monomer and template concentrations.[52] In this work, we extended this model to include monomer dimerization and examine its effects on numbers of background and templated binding sites (Scheme 2b).[41,42]

The equilibriums in the prepolymerization solution were modeled using the open source program COPASI, which was developed to simulate complex biological equilibrium and rate processes.[51] The imprinting simulation were based on four equilibria (eqs 1−4), which describe the ability of the monomer (M) to dimerize (eq 1) and to form 1:1, 2:1, and 3:1 complexes with the template (T). Each of these processes had a separate equilibrium constant (K_{dim}, K_{a1}, K_{a2}, K_{a3}). Thus, the input parameters for the simulations were K_{dim}, K_{a1}, K_{a2}, K_{a3}, [monomer], and [template]. The outputs of the simulations were the equilibrium concentrations of the various species in the prepolymerization solution which include [monomer], [dimer], [M_1T], [M_2T], and [M_3T].

For the initial simulations, the input parameters were based on the concentrations of monomer (0.2 M) and template (0.02 M) used in the experimental studies. The values for the dimerization and monomer−template association constants were based on the experimentally measured values in acetonitrile. The K_{dim} values used in the simulation were taken directly from the experimentally MAA dimerization constant. For the simulated MIP, the values for K_{a1}, K_{a2}, and K_{a3} were extrapolated from the experimental monomer−template association constant ($K_{a(exp)} = 7.5\ M^{-1}$) using eq 5 in which $K_{a(exp)}/3 = K_{a1}/3 = K_{a2} = 3K_{a3}$. For the simulated NIP, a much lower value of K_{a1} of 1.0 M^{-1} was used to model conditions where the monomer has no or very low affinity for the template. The template was not removed from the NIP simulation because it is known that the monomers in NIPs can randomly form high-affinity binding sites even in the absence of template. To model this behavior, we calculated the concentrations of monomer−template complexes that form with very low monomer−template association constants.[52]

Our first goal was to demonstrate that the equilibrium model was able to replicate the experimentally observed trends. To simplify the analyses, the four different types of binding sites in the simulation were divided up into two categories: selective and background binding sites. The selective sites were defined as those formed by the template and thus was equal to the sum of [M_1T], [M_2T], and [M_3T] in the prepolymerization solution. The number of background binding sites was defined as those formed without template and thus was equal to the concentration of free monomer, [monomer]. Binding sites formed from monomer dimers were considered to have no binding affinity and were not included in either category.

First, an MIP and NIP were simulated without monomer dimerization, and the numbers of each type of site were

Table 4. Numbers of Each Type of Binding Site in the Simulated MIPs and NIPs[a]

entry	simulated polymer	total no. of sites	no. of selective binding sites	no. of background binding sites	no. of dimerized binding sites
1	MIP without dimerization	0.195	0.0135 (7%)	0.181 (93%)	
2	NIP without dimerization	0.199	0.0035 (1.7%)	0.196 (98.3%)	
3	MIP with dimerization	0.135	0.0111 (8%)	0.124 (92%)	0.0308
4	NIP with dimerization	0.132	0.0024 (1.8%)	0.130 (98.2%)	0.0338

[a] The percentages of each type of binding sites are shown in parentheses. The dimerized sites were assumed to have no affinity and were not included in the total number of sites.

tabulated (Table 4, entries 1 and 2). A clear imprinting effect was observed as the MIP had a 4.5-fold higher number of selective binding sites than the NIP. The simulated polymers also shared other characteristics of experimental MIPs. For example, the selective sites in the simulated MIP and NIP represent only a small of a fraction of the total number of sites (7% and 1.7%). This is in agreement with studies of MIPs that have found that less than 10% of binding sites are selective sites due to the large excess of functional monomer that is used in their preparation.[20] These parallels between the simulated and experimental polymers along with our previous studies of simulated imprinted polymers[52] suggested that the association constants and general parameters provided a reasonable predictive model of the imprinting process.

Next, monomer dimerization was added to the model, and the effects on the numbers of binding sites were assessed (Table 4, entries 3 and 4). Despite the very low dimerization constant that was used in this simulation (K_{dim} = 1.9 M^{-1}), a significant fraction of monomer (~33%) was sequestered in the dimer due to the very high concentrations of monomer (0.2 M) used in the imprinting process. One consequence of monomer dimerization was that less monomer was available to form the selective and background binding sites. Interestingly, the effects were very similar for the MIP and NIP. In both cases, the polymers simulated with dimerization showed a 30% drop in total number of sites.

To test the accuracy of the dimerization model, we attempted to reproduce the results from the experimental studies in which the imprinting and dimerization processes were systematically disrupted by the addition of polar solvent to the prepolymerization solution. The effects of the polar solvents on the prepolymerization equilibriums were simulated by dividing the monomer−template association constants (K_{a1}, K_{a2}, and K_{a3}) and the dimerization constant (K_{dim}) by a common factor (s). The additions of increasing concentrations of polar solvents were simulated by increasing the factor s, which systematically weakened the monomer−template and dimer complexes. The overall binding capacities (B) of the simulated polymers were calculated using the bi-Langmuir model (eq 6) in which the two types of sites are the selective and background sites.[52,62]

$$B = N_S K_S F/(1 + K_S F) + N_B K_B F/(1 + K_B F) \qquad (6)$$

The values for the numbers of selective (N_S) and background (N_B) sites were calculated from the MIP and NIP simulations. Values for the association constants for the selective (K_S = 100 M^{-1}) and background (K_B = 10 M^{-1}) were based on the experimental 1:1 MAA−EA9A association constant. The background sites with one monomer recognition unit should have a similar association constant (K_B) as MAA for the template (~10^1 M^{-1}), and the selective sites have binding affinities (K_S) 1 order of magnitude higher. Note that these estimates are also consistent with experimentally measured association constants for the background and selective sites in EA9A MIPs.[45−47] The binding capacities (B) of the simulated polymers were calculated for a 0.1 mM analyte solution, which was the analyte concentration in the binding studies of the polymers.

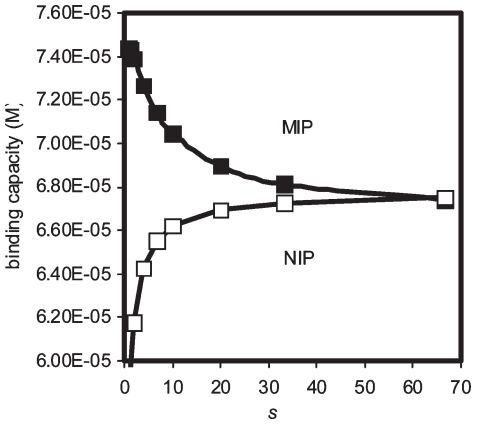

Figure 6. Calculated binding capacities of the simulated MIPs and NIPs formed under conditions in which the monomer−template association and monomer−monomer dimerization processes have been systematically disrupted as measured by the factor s.

The absolute values for B (in eq 6) are difficult to directly compare to the experimental binding capacities because the measured binding capacities provide only a lower estimate of the true numbers of binding sites in the polymers. Despite these differences, the overall trends for the binding capacities of the simulated MIP and NIP formed in increasingly polar solvents (Figure 6) were very similar to those observed in the experimental studies (Figure 3). As the association processes are increasingly disrupted with increasing S, the binding capacity of the MIP asymptotically decreases. The NIP, however, shows the exact opposite trend as its binding capacity asymptotically increases. The simulated MIPs and NIPs also converge at an intermediate binding capacity just like the experimental polymers. The similarities between the simulated and experimental results suggested that the monomer dimerization model was a reasonably accurate predictive model.

The value of the model was that it provides insight into the origins of the observed trends, as the numbers of each type of binding site can be easily calculated and compared. We were interested in three questions: (1) Are the higher binding capacities of the NIPs formed in more polar solvents due to ability of monomer dimerization to suppress the formation of background binding sites? (2) How efficiently does monomer dimerization also suppress the formation of background sites in the MIP? (3) Finally, what is the effect of monomer dimerization on ratio of selective to background sites?

First, the numbers of background binding sites was tabulated for the NIPs formed with varying s factors. As s increased, the number of background binding sites (filled squares) increased (Figure 7) in a similar asymptotic fashion to the experimentally observed increases in NIP binding capacity. The dramatic increases in the numbers of background binding sites can be directly linked to the disruption of the monomer dimers as hypothesized. As shown in Figure 7, the number of dimers (empty squares) shows a similar asymptotic decrease over the same range of s values.

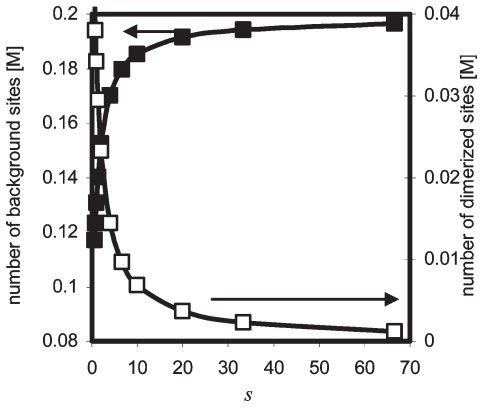

Figure 7. Numbers of background sites (filled squares) and number of dimer sites (empty squares) in a series of simulated NIPs in which monomer dimerization has been systematically disrupted as measured by the factor *s*.

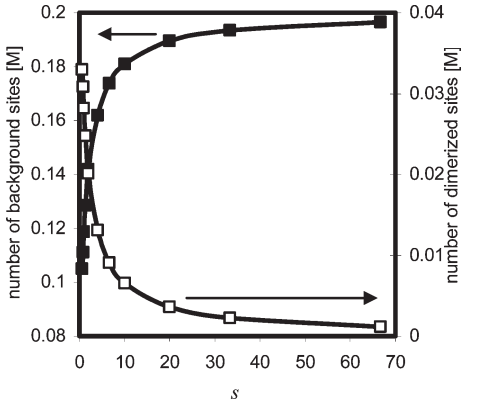

Figure 8. Number of background sites (filled squares) and number of dimer sites (empty squares) in a series of simulated MIPs in which monomer dimerization has been systematically disrupted as measured by the factor *s*.

To answer the second question, a similar analysis of the number of binding sites in the simulated MIP was conducted. Although the overall binding capacity of the simulated MIPs decreased with increasing *s* values, the number of background binding sites actually increased dramatically just like in the NIP (Figure 8, filled squares). The increase in the number of background sites can be directly correlated to the decrease in the number of monomer dimers with increasing *s*, confirming that monomer dimerization also suppressed the formation of background sites in the MIP. The magnitude of the effect was very similar in MIP and NIP as numbers of dimers in the MIP and NIP are very similar (Table 4).

Finally, the impact of monomer dimerization on the overall binding properties of the MIPs was assessed. Although the numbers of each type of site decreased with increasing monomer dimerization, we hypothesized that the overall effect of monomer dimerization could still be beneficial if the number of background sites decreased faster than the number of templated sites. In the EA9A MIPs, the monomer−template association constant was higher than the monomer−monomer dimerization constant. Therefore, the templation processes should be able to outrival monomer dimerization process.

To test this hypothesis, the relative numbers of selective and background sites were compared in the MIPs formed with and without monomer dimerization (Table 4, entries 3 and 1). As expected, the numbers of selective and background sites were lower in the MIP with dimerization. However, the percent decrease of each type of site was

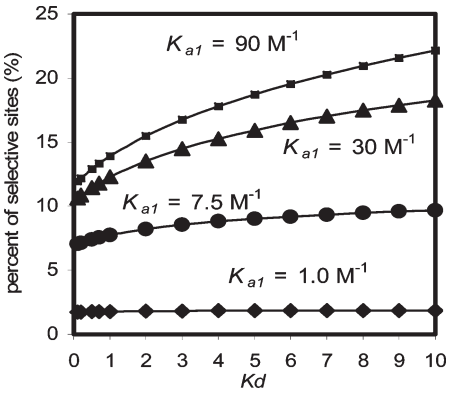

Figure 9. Comparison of the percentage of selective sites in simulated MIPs of varying template−monomer association constants and with varying monomer dimerization constants.

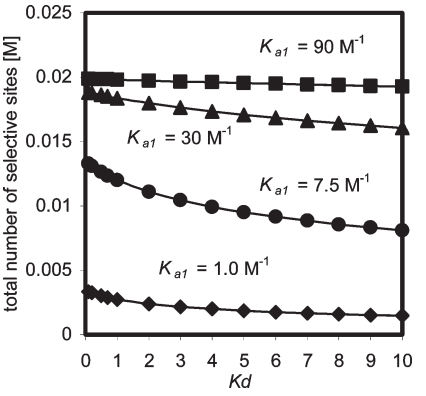

Figure 10. Comparison of total number of selective sites in simulated MIPs of varying template−monomer association constants and with varying monomer dimerization constants.

similar, leading to very similar percentage of sites in both MIPs (with and without dimerization). This suggests that, at worst, monomer dimerization does not change the ratio of selective to background sites in MIPs. Closer examination of the percentages showed that dimerization slightly improved the selectivity as the MIP with dimerization had a slightly higher percentage of selective sites (8% vs 7%).

To test whether this small increase in the percentage of selective sites was statistically relevant, the percentages of selective sites were simulated for MIPs having a wide range of dimerization and monomer−template association constants (Figure 9). Higher percentages of selective sites formed using higher monomer−template association constants (K_{a1}), which was consistent with the imprinting process. More interestingly, the percentage of selective sites increased with increasing K_{dim}. The largest improvements in percentages of selective sites were observed for the MIPs with higher monomer−template association constants. This is reasonable for the competition of templation and dimerization: the stronger the templation, the more monomer will form templated sites; thus, the percentage of selective sites increased. For example, for the simulated MIPs with K_{a1} = 90 M^{-1}, the percentage of selective sites increased from 12% to 22%. However, even the simulated MIPs with the lowest monomer−template association constants (K_{a1} = 1.0 M^{-1}) showed modest improvements in the percentages of selective sites at higher K_{dim} (from 1.7% to 1.9%)

While the data in Figure 10 suggest that higher values of K_{dim} are always preferable, this analysis does not take into account the overall decreases in binding capacities of the

polymers. As shown in Figure 10, the total number of selective sites in the MIPs decreased with increasing K_{dim}. For example, for $K_{a1} = 1.0\ M^{-1}$, the number of selective sites decreased from 0.0034 to 0.0015, and for $K_{a1} = 90\ M^{-1}$, the number of selective sites decreased from 0.020 to 0.019. Therefore, the optimal K_{dim} values will depend upon the target application. For applications such as sensing where selectivity is of great importance, polymers formed with monomer with higher dimerization constants would be beneficial. However, for applications were binding capacity is of greater importance such as solid-phase extraction or chromatography, an intermediate value of K_{dim} would yield a better balance of optimal selectivity and binding capacity.

In summary, the computer simulations predicted that monomer dimerization was equally effective in suppressing the formation of background sites in MIPs as in NIPs. Monomer dimerization also reduced the number of templated selective sites. However, these detrimental effects can be mitigated by choosing monomers that form stronger complexes with the prospective templates. This approach of reducing the number of background sites is of practical utility as the high percentages of background sites in MIPs have been shown to be a contributing source to many of their undesirable properties. These include the extreme peak asymmetry of MIP chromatographic stationary phases and the poor overall binding affinities and selectivities of MIP recognition materials.[34,52,61]

Conclusions

MAA dimerization was shown to effectively reduce the number of background sites in MIPs both in experiment and simulation. MAA dimerization also reduced the number of templated sites, but the overall effect was beneficial as the number of background sites was reduced by a large percentage. Simulations predict that for monomers that form stronger monomer−template interactions the monomer dimerization can actually improve the imprinting efficiency as measured by the fraction of selective templated and background sites. Both our experimental and simulation results help explain why MAA was such a versatile monomer for molecular imprinting. The results revealed that the dimerization of MAA modestly enhanced the imprinting effect. However, the polymers in this study were formed using thermal initiation methods. Polymers formed at lower temperatures using photochemical initiation methods should show even larger effects as the association processes will be should be stronger at lower temperatures. On the basis of these studies with MAA, we predict that other functional monomers that can dimerize or aggregate should also show higher imprinting efficiencies in terms of selectivity while sacrificing some binding capacity. Finally, both experimental and simulation results demonstrated that one must be very careful when using NIPs as control systems to characterize the imprinting effect as the suppression of background sites in the NIP can lead to differences in binding capacities of the MIP and NIP even in the absence of an imprinting effect.

Acknowledgment. The authors thank the National Science Foundation (0828897) for financial support.

Supporting Information Available: Additional data for the COPASI simulations and BET measurements. This material is available free of charge via the Internet at http://pubs.acs.org.

References and Notes

(1) Wulff, G. *Chem. Rev.* **2002**, *102*, 1–27.
(2) Yan, M.; Ramstrom, O. *Molecularly Imprinted Materials: Science and Technology*; Marcel Dekker: New York, 2005; pp 1−123.
(3) Sellergren, B. *Molecularly Imprinted Polymers: Man-Made Mimics of Antibodies and Their Applications in Analytical Chemistry*; Elsevier: Amsterdam, 2001; p 557.
(4) Zimmerman, S. C.; Wendland, M. S.; Rakow, N. A.; Zharov, I.; Suslick, K. S. *Nature* **2002**, *418*, 399.
(5) Kriz, D.; Mosbach, K. *Anal. Chim. Acta* **1995**, *300*, 71–75.
(6) Kroger, S.; Turner, A. P.; Mosbach, K.; Haupt, K. *Anal. Chem.* **1999**, *71*, 3698–3702.
(7) Andersson, L. I. *Anal. Chem.* **1996**, *68*, 111–117.
(8) Andersson, L. I.; O'Shannessy, D. J.; Mosbach, K. *J. Chromatogr. A* **1990**, *513*, 167–169.
(9) Ramstrom, O.; Nicholls, I. A.; Mosbach, K. *Tetrahedron: Asymmetry* **1994**, *5*, 649–656.
(10) Kempe, M.; Mosbach, K. *J. Chromatogr. A* **1995**, *691*, 317–323.
(11) Shea, K. J.; Spivak, D. A.; Sellergren, B. *J. Am. Chem. Soc.* **1993**, *115*, 3368–3369.
(12) Zimmerman, S. C.; Lemcoff, N. G. *Chem. Commun.* **2004**, *7*, 5–14.
(13) Svenson, J.; Nicholls, I. A. *Anal. Chim. Acta* **2001**, *435*, 19–24.
(14) Fischer, L.; Mueller, R.; Ekberg, B.; Mosbach, K. J. *J. Am. Chem. Soc.* **1991**, *113*, 9358–9360.
(15) Spivak, D. A.; Shea, K. J. *Macromolecules* **1998**, *31*, 2160–2165.
(16) Alvarez-Lorenzo, C.; Concheiro, A. *J. Chromatogr. B* **2004**, *804*, 231–245.
(17) Bjarnason, B.; Chimuka, L.; Ramstrom, O. *Anal. Chem.* **1999**, *71*, 2152–2156.
(18) Zander, A.; Findlay, P.; Renner, T.; Sellergren, B.; Swietlow, A. *Anal. Chem.* **1998**, *70*, 3304–3314.
(19) Haupt, K.; Mosbach, K. *Chem. Rev.* **2000**, *100*, 2495–2504.
(20) Umpleby, R. J.; Bode, M.; Shimizu, K. D. *Analyst* **2000**, *125*, 1261–1265.
(21) Umpleby, R. J.; Baxter, S. C.; Bode, M.; Berch, J. K.; Shah, R. N.; Shimizu, K. D. *Anal. Chim. Acta* **2001**, *435*, 35–42.
(22) Rampey, A. M.; Umpleby, R. J.; Rushton, G. T.; Iseman, J. C.; Shah, R. N.; Shimizu, K. D. *Anal. Chem.* **2004**, *76*, 1123–1133.
(23) Kempe, M. *Anal. Chem.* **1996**, *68*, 1948–1953.
(24) Yilmaz, E.; Haupt, K.; Mosbach, K. *Anal. Commun.* **1999**, *36*, 167–170.
(25) Wulff, G.; Vietmeier, J.; Poll, H. G. *Makromol. Chem.* **1987**, *188*, 731–740.
(26) O'Shannessy, D. J.; Ekberg, B.; Mosbach, K. *Anal. Biochem.* **1989**, *177*, 144–149.
(27) Chen, Y.; Kele, M.; Sajonz, P.; Sellergren, B.; Guiochon, G. *Anal. Chem.* **1999**, *71*, 928–938.
(28) Sellergren, B. *J. Chromatogr. A* **1994**, *673*, 133–141.
(29) Sellergren, B.; Shea, K. J. *J. Chromatogr.* **1993**, *635*, 31–49.
(30) Mosbach, K.; Ramstrom, O. *Bio/Technol.* **1996**, *14*, 163–170.
(31) Kandimalla, V. B.; Ju, H. *Anal. Bioanal. Chem.* **2004**, *380*, 587–605.
(32) Alexander, C.; Andersson, H. S.; Andersson, L. I.; Ansell, R. J.; Kirsch, N.; Nicholls, I. A.; O'Mahony, J.; Whitcombe, M. J. *J. Mol. Recognit.* **2006**, *19*, 106–180.
(33) Stephenson, C. J.; Shimizu, K. D. *Polym. Int.* **2007**, *56*, 482–488.
(34) Wulff, G. *Angew. Chem., Int. Ed. Engl.* **1995**, *34*, 1812–1832.
(35) Haupt, K.; Mosbach, K. *Trends Biotechnol.* **1998**, *16*, 468–475.
(36) Santora, B. P.; Gagné, M. R.; Moloy, K. G.; Radu, N. S. *Macromolecules* **2001**, *34*, 658–661.
(37) Peters, E. C.; Svec, F.; Frechet, J. M. J. *Adv. Mater.* **1999**, *11*, 1169–1181.
(38) Malosse, L.; Palmas, P.; Buvat, P.; Ades, D.; Siove, A. *Macromolecules* **2008**, *41*, 7834–7842.
(39) Ansell, R. J.; Kuah, K. L. *Analyst* **2005**, *130*, 179–187.
(40) Chen, J.-S. *J. Chem. Soc., Faraday Trans.* **1994**, *90*, 717–720.
(41) Ansell, R. J.; Wang, D. Y.; Kuah, J. K. L. *Analyst* **2008**, *133*, 1673–1683.
(42) Ansell, R. J.; Wang, D. Y. *Analyst* **2009**, *134*, 564–576.
(43) Wu, X.; Goswami, K.; Shimizu, K. D. *J. Mol. Recognit.* **2008**, *21*, 410–418.
(44) Allender, C. J. *Adv. Drug Delivery Rev.* **2005**, *57*, 1731–1732.
(45) Degenhardt, C. F.; Lavin, J. M.; Smith, M. D.; Shimizu, K. D. *Org. Lett.* **2005**, *7*, 4079–4081.
(46) Lavin, J. M.; Shimizu, K. D. *Org. Lett.* **2006**, *8*, 2389–2392.
(47) Spivak, D.; Gilmore, M. A.; Shea, K .J. *J. Am. Chem. Soc.* **1997**, *119*, 4388–4393.
(48) Rao, P.; Ghosh, S.; Maitra, U. *J. Phys. Chem. B* **1999**, *103*, 4528–4533.
(49) Connors, K. A. *Binding Constants: The Measurement of Molecular Complex Stability*; Wiley: New York, 1987.

(50) Williams, D. H.; Gale, T. F.; Bardsley, B. *J. Chem. Soc., Perkin Trans. 2* **1999**, 1331–1334.
(51) Hoops, S.; Sahle, S.; Gauges, R.; Lee, C.; Pahle, J.; Simus, N.; Singhal, M.; Xu, L.; Mendes, P.; Kummer, U. *Bioinformatics* **2006**, *22*, 3067–3074.
(52) Wu, X.; Carroll, W. R.; Shimizu, K. D. *Chem. Mater.* **2008**, *20*, 4335–4346.
(53) Whitcombe, M. J.; Martin, L.; Vulfson, E. N. *Chromatographia* **1998**, *47*, 457–464.
(54) Karle, J.; Brockway, L. O. *J. Am. Chem. Soc.* **1944**, *66*, 574.
(55) Barrow, G. M.; Yerger, E. A. *J. Am. Chem. Soc.* **1954**, *76*, 5248–5249.
(56) Doan, V.; Koeppe, R.; Kasai, P. H. *J. Am. Chem. Soc.* **1997**, *119*, 9810–9815.
(57) Dong, J.; Ozaki, Y.; Nakashima, K. *Macromolecules* **1997**, *30*, 1111–1117.
(58) Santora, B. P.; Gagne, M. R.; Moloy, K. G.; Radu, N. S. *Macromolecules* **2001**, *34*, 658–661.
(59) Matsui, J.; Kubo, H.; Takeuchi, T. *Anal. Sci.* **1998**, *14*, 699–702.
(60) Karlsson, J. G.; Karlsson, B.; Andersson, L. I.; Nicholls, I. A. *Analyst* **2004**, *129*, 456–462.
(61) Rushton, G. T.; Karns, C. L.; Shimizu, K. D. *Anal. Chim. Acta* **2005**, *528*, 107–113.
(62) Umpleby, R. J., II; Baxter, S. C.; Rampey, A. M.; Rushton, G. T.; Chen, Y.; Shimizu, K. D. *J. Chromatogr. B* **2004**, *804*, 141–149.
(63) Srebnik, S.; Lev, O. *J. Chem. Phys.* **2002**, *116*, 10967–10972.
(64) Yungerman, I.; Srebnik, S. *Chem. Mater.* **2006**, *18*, 657–663.
(65) Srebnik, S. *Chem. Mater.* **2004**, *16*, 883–888.
(66) Wu, L. Q.; Sun, B. W.; Li, Y. Z.; Chang, W. B. *Analyst* **2003**, *128*, 944–949.
(67) Piletsky, S. A.; Karim, K.; Piletska, E. V.; Day, C. J.; Freebairn, K. W.; Legge, C.; Turner, A. P. F. *Analyst* **2001**, *126*, 1826–1830.
(68) Takeuchi, T.; Dobashi, A.; Kimura, K. *Anal. Chem.* **2000**, *72*, 2418–2422.
(69) Wei, S.; Jakusch, M.; Mizaikoff, B. *Anal. Bioanal. Chem.* **2007**, *389*, 423–431.